

# Machine learning-based prediction of 5-year survival in diffuse-type gastric cancer patients from Harbin

Yongle Zhang<sup>#</sup>, Cong Wang<sup>#</sup>, Jiale Fan, Hongyu Gao, Xiqing Zhu<sup>\*</sup>, Haibin Song<sup>\*</sup>

## Abstract

**Objective:** Globally, over 1.1 million new cases of gastric cancer (GC) were diagnosed in 2020, with approximately 800,000 related deaths. GC exhibits significant regional variability, particularly in extremely cold regions, where unique climate conditions and lifestyle factors may impact disease progression and prognosis. This study aimed to predict the 5-year all-cause mortality of patients with diffuse gastric cancer (DGC) living in such regions using multiple machine learning algorithms. **Methods:** We retrospectively analyzed 249 DGC cases and developed six machine learning models—extreme gradient boosting (XGBoost), logistic regression, decision tree, support vector machine, k-nearest neighbors, and random forest. Model performance was assessed using the area under the receiver operating characteristic curve (AUC), precision-recall curve, F1 score, and Brier score. **Results:** The XGBoost model achieved the highest F1 scores (0.830 and 0.781, respectively) and the second-best Brier score (0.172). **Conclusion:** This study highlights the potential of machine learning approaches to enhance prognostic assessment in GC. Although limited by single-center data and the absence of multi-center external validation, the results offer valuable insights that may inform future research and guide risk-stratified management strategies in extremely cold regions.

## Keywords

gastric cancer; XGBoost; cold region

Received 09 August 2024, accepted 04 November 2024

Department of Gastroenterological Surgery, Harbin Medical University Cancer Hospital, Harbin Medical University, Harbin 150000, China

<sup>#</sup>These authors contributed equally to this work.

<sup>\*</sup>Corresponding authors Haibin Song, E-mail:601484@hrbmu.edu.cn; Xiqing Zhu, E-mail: 2022021780@hrbmu.edu.cn

Open Access. © 2026 The author (s), published by De Gruyter on behalf of Heilongjiang Health Development [CC BY] Research Center. This work is licensed under the Creative Commons Attribution 4.0 International License.

## 1 Introduction

Globally, more than 1.1 million new cases of gastric cancer (GC) were diagnosed in 2020, with approximately 800,000 related deaths. Notably, around 75% of these cases and deaths occurred in Asia. The overall 5-year survival rate remains around 20%, placing GC as the fifth most common malignancy and the fourth leading cause of cancer-related mortality<sup>[1-3]</sup>. Despite advances in surgical techniques, radical gastrectomy remains the primary treatment for GC; however, the long-term survival rate still falls below 30%<sup>[4-7]</sup>.

The Lauren classification system, introduced in 1965, is a widely used histological framework categorizing GC into intestinal, diffuse, and mixed subtypes<sup>[8]</sup>. The intestinal subtype consists of cohesive cells that arrange into gland-like structures, whereas the diffuse subtype is characterized by non-cohesive tumor cells that infiltrate the stroma individually or in small clusters<sup>[8]</sup>. Mixed-type GC displays features of both. The Lauren classification plays

a significant role as a prognostic indicator for GC patients<sup>[9]</sup>. Previous studies have shown that patients with diffuse gastric cancer (DGC) have markedly lower five-year overall survival compared to those with intestinal gastric cancer (IGC), and multi-variable analyses have confirmed Lauren classification as an independent negative prognostic factor<sup>[10]</sup>. Additional evidence indicates that DGC is associated with greater aggressiveness and a higher likelihood of lymph node metastasis, contributing to poorer prognosis<sup>[11]</sup>. For patients with an inherently poor prognosis, tailoring treatment strategies according to expected survival time becomes crucial. Hence, predicting the survival period of DGC patients may help guide more individualized clinical decision-making.

GC also exhibits substantial regional differences worldwide. In this study, "extremely cold regions" refer to geographical areas where the average annual temperature is significantly lower than the national mean—for example, Harbin and surrounding areas in China, where the annual temperature typically ranges from -5 °C

to -4 °C. In such environments, climate characteristics, dietary patterns, and lifestyle behaviors may uniquely influence GC incidence and mortality. Harsh climatic conditions often lead to dietary changes, including increased consumption of high-salt and pickled foods, both recognized risk factors for GC<sup>[12]</sup>, as supported by previous reports<sup>[13]</sup>. Additionally, prolonged exposure to cold environments may affect immune system function and thereby influence the development and progression of GC<sup>[14]</sup>.

Artificial intelligence (AI) is an emerging technical discipline focused on developing theories, methods, and applications that simulate or extend human intelligence. In recent years, machine learning—one of the core branches of AI—has been widely applied to various medical fields, particularly for predictive modeling, with promising performance<sup>[15-17]</sup>. Although multiple studies have explored machine learning applications in GC prediction, an important gap remains: the prediction of 5-year all-cause mortality specifically for patients with DGC<sup>[18]</sup>.

This study aims to apply several machine learning models to predict the 5-year all-cause mortality of DGC patients living in extremely cold regions and to compare model performance in order to identify the optimal predictive approach.

## 2 Methods and patients

### 2.1 Patient selection

This retrospective study included 249 patients diagnosed with DGC at the Affiliated Tumor Hospital of Harbin Medical University between 2014 and 2018. Patients were selected according to predefined exclusion criteria. This study was conducted in accordance with the principles of the Declaration of Helsinki and was approved by the Medical Ethics Committee of Harbin Medical University Cancer Hospital (KY2021-09). Informed consent was obtained from all patients prior to treatment.

The exclusion criteria were as follows: (1) patients who received neoadjuvant therapy or conversion therapy ( $N = 7$ ); (2) patients with concurrent malignancies ( $N = 3$ ); (3) individuals with multifocal gastric cancer ( $N = 1$ ); (4) patients who declined or refused treatment for various reasons ( $N = 2$ ).

### 2.2 Study outcome

The primary endpoint was the 5-year all-cause mortality among patients with DGC. Secondary outcomes included risk stratification based on prediction scores and comparison of survival differences between high-risk and low-risk groups using Kaplan-Meier analysis.

### 2.3 Feature selection and data preprocessing

For variables with missing data rates up to 30%, missing values were imputed using the K-Nearest Neighbors Imputer<sup>[19]</sup>. Polychotomous variables were processed using One-Hot encoding<sup>[20]</sup>. To determine the most informative predictors for model construction, recursive feature elimination (RFE) was applied to select a final subset of 10 features. RFE works by iteratively fitting a model, ranking features by importance, removing the least important feature, and repeating this process until all features have been assessed.

### 2.4 Model development

Six machine learning models were developed to predict the 5-year all-cause mortality of GC patients: extreme gradient boosting (XGBoost), logistic regression (LR), decision tree (DT), support vector machine (SVM), k-nearest neighbors (KNN), and random forest (RF). XGBoost is a highly efficient algorithm suitable for regression and classification tasks, offering strong predictive accuracy and low computational costs<sup>[21]</sup>. LR models are frequently utilized to evaluate the influence of predictor variables on binary variables<sup>[22]</sup>. DT is one of the earliest machine learning algorithms and represents mappings between object attributes and their corresponding values; each internal node denotes an attribute, each branch indicates a decision rule, and each leaf node represents an output value<sup>[23]</sup>. RF is an ensemble classifier that improves predictive stability and generalization through the aggregation of multiple decision trees<sup>[24]</sup>. SVM is effective for separating samples with multidimensional attributes into two classes<sup>[25]</sup>. KNN is a widely used non-parametric method based on the assumption that a sample can be classified according to the predominant class among its  $k$  nearest neighbors<sup>[26]</sup>.

The patient cohort was randomly divided into a training set and a test set in a 7 : 3 ratio. A 10-fold cross-validation strategy was applied within the training set to enhance model robustness and minimize overfitting. The training set was utilized to construct all machine learning models, whereas the test set served to evaluate their predictive performance.

The optimal model among the six models was identified by comparing multiple evaluation metrics and was then applied for subsequent risk prediction and stratification (Fig. 1).

### 2.5 Statistical analysis

All statistical analyses were performed using R software (version 4.2.3) and Python (version 3.9). Categorical variables were summarized as frequencies and percentages, and differences between groups were assessed using either the chi-squared test

or Fisher's exact test, as appropriate. Continuous variables were described using median and mean values, accompanied by inter-quartile range (IQR) and standard deviation (SD).

Model performance was evaluated comprehensively using the Area under the Receiver Operating Characteristic Curve (AUC), Precision-Recall curve (PR), F1 score, and sensitivity. Model calibration was assessed with the Brier score. The optimal cutoff value for distinguishing high-risk from low-risk patients was determined using the maximum Youden index. The Kaplan-Meier method and log-rank test were subsequently applied to compare survival curves between the two risk groups. All statistical tests were two-sided, and a significance level  $< 0.05$  was considered statistically significant.

## 3 Results

### 3.1 Patient baseline

A total of 249 patients with DGC were included in this study, with 174 assigned to the training set and 75 to the test set. No significant differences were observed between the two groups with respect to gender, age, tumor size, lymph node metastasis, distant metastasis, general type, survival duration, histological subtype, or other baseline characteristics. This indicates that the patient distribution between the training and test sets was well balanced (Table 1).

### 3.2 Feature selection

Using recursive elimination, 10 optimal predictors were identified:

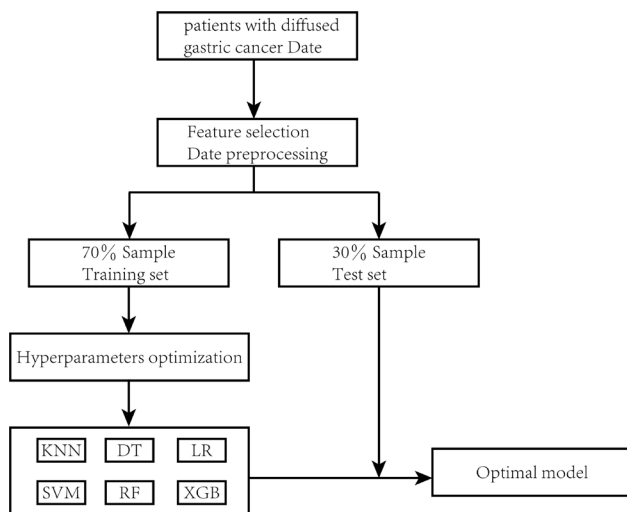


**Fig. 1** Flow chart for the development, explanation and validation of models KNN, k-nearest neighbors; DT, decision tree; LR, logistic regression; SVM, support vector machine; RF, random forest; XGB, extreme gradient boosting.

pathological T stage (pT), pathological N stage (pN), pathological TNM stage (pTNM), lymphocyte count (LYM), red blood cell count (RBC), alkaline phosphatase (ALP), total bilirubin (TBIL), carbohydrate antigen 19-9 (CA19-9), carbohydrate antigen 125 (CA125), and the presence of Borrmann type IV gastric cancer (Fig. 2).

### 3.3 Predictive abilities of different ML models

The predictive performance of the six ML models was compared using AUC, PR curve, F1 score, and sensitivity. The XGBoost model demonstrated the strongest overall performance. It achieved the highest AUC in both the training set (0.887, SD = 0.06; Fig. 3A) and the test set (0.820, 95% CI 0.805-0.833; Fig. 3B), and its calibration curve closely approximated the ideal calibration line (Fig. 3C).

In the test set, the RF model had the lowest Brier score (0.170, 95% CI 0.163-0.176), followed closely by the XGBoost model with a Brier score of 0.172 (95% CI 0.166-0.177), ranking second (Fig. 3C). The XGBoost model also achieved the highest F1 score in the test set (0.781; Table 2), while its F1 score in the training set was 0.83 (SD = 0.07; Table 3), ranking third.

Moreover, XGBoost exhibited the highest PR value among all six models, with a value of 0.824 (Fig. 3D). Based on a comprehensive comparison of performance metrics across all models, XGBoost was identified as the optimal model for predicting the 5-year all-cause mortality of DGC patients.

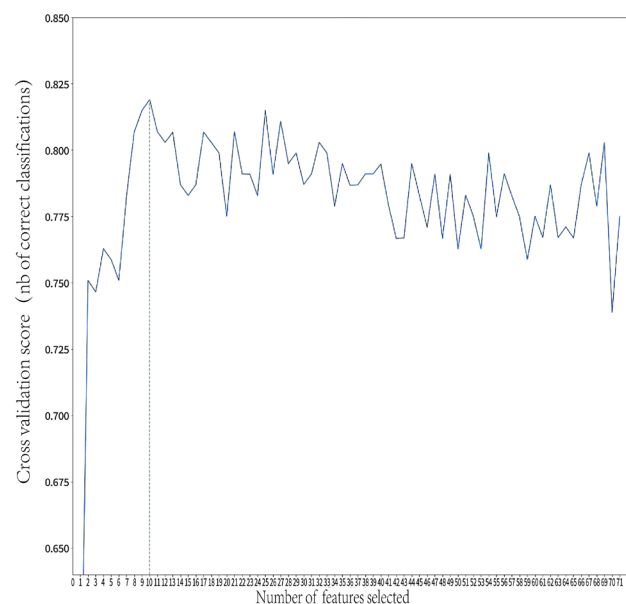


**Fig. 2** Results of feature screening using recursive feature elimination with 10-fold cross-validation

Table 1 Baseline demographics and clinical characteristics of the study population

Characteristics	Level	Overall (N = 249)	Test set (N = 75)	Training set (N = 174)	P value
Status					1.000
Survival		103 (41.4)	31 (41.3)	72 (41.4)	
Death		146 (58.6)	44 (58.7)	102 (58.6)	
Sex					0.422
Female		144 (57.8)	40 (53.3)	104 (59.8)	
Male		105 (42.2)	35 (46.7)	70 (40.2)	
Radical	Yes	194 (77.9)	59 (78.7)	135 (77.6)	0.982
	No	55 (22.1)	16 (21.3)	39 (22.4)	
pT	T1	8 (3.2)	4 (5.3)	4 (2.3)	0.527
	T2	19 (7.6)	5 (6.7)	14 (8.0)	
	T3	133 (53.4)	37 (49.3)	96 (55.2)	
	T4	89 (35.7)	29 (38.7)	60 (34.5)	
pN	N1	51 (20.5)	15 (20.0)	36 (20.7)	0.452
	N2	51 (20.5)	13 (17.3)	38 (21.8)	
	N3a	105 (42.2)	37 (49.3)	68 (39.1)	
	N3b	42 (16.9)	10 (13.3)	32 (18.4)	
pTNM	I	17 (6.8)	5 (6.7)	12 (6.9)	0.916
	II	67 (26.9)	18 (24.0)	49 (28.2)	
	III	153 (61.4)	48 (64.0)	105 (60.3)	
	IV	12 (4.8)	4 (5.3)	8 (4.6)	
Borrmann	0	6 (2.4)	2 (2.7)	4 (2.3)	0.431
	I	2 (0.8)	0 (0.0)	2 (1.1)	
	II	42 (16.9)	9 (12.0)	33 (19.0)	
	III	128 (51.4)	44 (58.7)	84 (48.3)	
	IV	59 (23.7)	15 (20.0)	44 (25.3)	
	V	12 (4.8)	5 (6.7)	7 (4.0)	
WHO Classification	Well-to-moderate differentiated	3 (1.2)	1 (1.3)	2 (1.1)	0.913
	Poorly differentiated	24 (9.6)	6 (8.0)	18 (10.3)	
	Signet-ring cell	14 (5.6)	5 (6.7)	9 (5.2)	
	Mucinous	208 (83.5)	63 (84.0)	145 (83.3)	
Location	Upper stomach	16 (6.4)	9 (12.0)	7 (4.0)	0.005
	Middle stomach	55 (22.1)	8 (10.7)	47 (27.0)	
	Lower stomach	133 (53.4)	46 (61.3)	87 (50.0)	
	Whole stomach	45 (18.1)	12 (16.0)	33 (19.0)	
Tumor Size (mm)		50.00 (35.00, 60.00)	50.00 (35.00, 60.00)	50.00 (35.00, 70.00)	0.423
Age (years)		54.00 (46.00, 61.00)	56.00 (46.00, 60.00)	54.00 (46.00, 62.00)	0.990
WBC ( $\times 10^9/L$ )		6.31 (5.21, 7.75)	6.27 (5.23, 7.58)	6.31 (5.22, 8.05)	0.776
LYM ( $\times 10^9/L$ )		1.82 (1.44, 2.27)	1.82 (1.47, 2.24)	1.83 (1.42, 2.28)	0.898
NEU ( $\times 10^9/L$ )		3.76 (2.78, 4.84)	3.55 (2.77, 4.42)	3.84 (2.81, 5.00)	0.306
MONO ( $\times 10^9/L$ )		0.46 (0.35, 0.61)	0.47 (0.36, 0.62)	0.46 (0.35, 0.60)	0.596
EOS ( $\times 10^9/L$ )		0.11 (0.06, 0.20)	0.12 (0.08, 0.24)	0.11 (0.06, 0.19)	0.059
BASO ( $\times 10^9/L$ )		0.02 (0.01, 0.04)	0.02 (0.01, 0.04)	0.02 (0.01, 0.04)	0.634
RBC ( $\times 10^{12}/L$ )		4.37 (4.03, 4.74)	4.35 (3.93, 4.71)	4.38 (4.06, 4.76)	0.583
HGB (g/L)		131.00 (110.00, 144.00)	132.70 (109.00, 143.00)	130.95 (111.00, 144.15)	0.916
HCT (%)		39.92 (34.80, 43.30)	40.42 (34.82, 43.81)	39.64 (34.60, 43.09)	0.912
MCV (fL)		90.80 (85.70, 94.10)	90.80 (86.50, 94.40)	90.60 (85.70, 93.80)	0.543
MCH (pg)		30.00 (28.00, 31.30)	29.90 (28.50, 31.30)	30.20 (27.90, 31.30)	0.706
MCHC (g/L)		327.00 (319.00, 335.00)	327.00 (319.00, 334.00)	327.00 (318.25, 335.00)	0.954
RDW (%)		13.20 (12.70, 14.20)	13.20 (12.65, 14.10)	13.20 (12.70, 14.20)	0.876
PLT ( $\times 10^9/L$ )		259.00 (211.00, 310.00)	272.00 (205.50, 329.50)	252.50 (213.00, 306.25)	0.498

Continued

Table 1Continued

Characteristics	Level	Overall (N = 249)	Test set (N = 75)	Training set (N = 174)	P value
MPV (fL)		9.70 (8.60, 10.50)	9.60 (8.60, 10.50)	9.70 (8.70, 10.50)	0.429
PDW (%)		15.90 (12.20, 16.50)	15.90 (12.95, 16.55)	15.90 (11.90, 16.50)	0.650
PCT (%)		0.25 (0.20, 0.31)	0.25 (0.20, 0.32)	0.25 (0.20, 0.30)	0.773
ALT (U/L)		17.00 (13.00, 24.00)	16.00 (12.50, 20.70)	17.00 (13.00, 25.00)	0.182
AST (U/L)		20.00 (17.00, 25.00)	20.00 (17.00, 24.00)	20.00 (17.00, 26.00)	0.480
γ-GGT (U/L)		15.50 (10.00, 24.00)	15.00 (9.00, 21.50)	16.00 (11.00, 24.00)	0.198
LDH (U/L)		158.00 (138.00, 177.00)	163.00 (143.50, 180.50)	155.50 (135.00, 173.00)	0.036
ALP (U/L)		73.00 (58.00, 87.00)	70.00 (54.00, 85.50)	74.50 (59.25, 87.00)	0.189
TBIL (μmol/L)		10.75 (7.90, 14.27)	12.06 (7.86, 14.85)	10.57 (7.93, 14.02)	0.275
DBIL (μmol)		3.90 (2.85, 5.07)	4.23 (3.06, 5.24)	3.83 (2.76, 4.97)	0.133
IDBIL (μmol/L)		6.92 (4.79, 9.36)	7.57 (5.03, 9.75)	6.65 (4.82, 8.89)	0.391
TP (g/L)		67.00 (63.00, 71.00)	66.00 (62.50, 71.00)	67.00 (63.00, 71.75)	0.474
ALB (g/L)		41.00 (37.00, 44.00)	41.00 (38.00, 44.00)	40.05 (37.00, 44.00)	0.609
GLOB (g/L)		26.00 (23.00, 29.00)	25.00 (22.00, 27.50)	26.00 (24.00, 29.00)	0.083
A/G		1.60 (1.40, 1.80)	1.60 (1.40, 1.80)	1.60 (1.40, 1.70)	0.220
PALB (mg/L)		241.00 (197.00, 285.00)	248.00 (196.00, 288.50)	239.00 (200.25, 282.00)	0.661
GLU (mmol/L)		5.00 (4.60, 5.50)	5.00 (4.50, 5.40)	4.95 (4.60, 5.57)	0.890
UREA (mmol/L)		5.30 (4.30, 6.40)	5.30 (3.90, 6.30)	5.35 (4.40, 6.50)	0.132
CREA (mmol/L)		75.00 (65.00, 84.00)	73.00 (63.00, 82.00)	76.00 (65.15, 85.00)	0.167
UA (mmol/L)		270.00 (227.00, 332.00)	264.00 (210.00, 314.50)	274.50 (234.00, 337.75)	0.123
CO <sub>2</sub> -CP (mmol/L)		28.70 (26.50, 30.40)	28.60 (27.20, 30.30)	28.75 (26.22, 30.48)	0.870
K (mmol/L)		4.27 (4.00, 4.49)	4.30 (4.04, 4.50)	4.24 (4.00, 4.47)	0.249
Na (mmol/L)		141.00 (139.00, 144.00)	142.00 (139.50, 143.50)	141.00 (139.00, 144.00)	0.840
CL (mmol/L)		104.00 (101.00, 106.00)	104.00 (101.00, 107.00)	104.00 (101.00, 106.00)	0.700
Ca (mmol/L)		2.30 (2.20, 2.40)	2.20 (2.10, 2.40)	2.30 (2.20, 2.40)	0.278
PHOS (mmol/L)		1.16 (1.05, 1.28)	1.18 (1.06, 1.31)	1.15 (1.05, 1.27)	0.272
Mg (mmol/L)		0.96 (0.11)	0.95 (0.11)	0.97 (0.11)	0.478
CA199 (U/mL)		9.12 (6.01, 17.95)	9.97 (6.34, 21.20)	8.84 (5.83, 16.27)	0.296
CEA (ng/mL)		1.63 (0.90, 2.93)	1.95 (1.00, 2.79)	1.54 (0.83, 3.04)	0.295
CA724 (U/mL)		2.47 (1.30, 6.72)	2.15 (1.29, 6.40)	2.74 (1.32, 7.85)	0.364
CA125 (U/mL)		10.51 (7.92, 15.70)	10.88 (8.03, 15.23)	10.18 (7.73, 15.75)	0.621
PH		6.00 (5.50, 6.50)	6.00 (5.50, 6.50)	6.00 (5.50, 6.50)	0.579
SG		1.02 (1.02, 1.03)	1.02 (1.01, 1.02)	1.02 (1.02, 1.03)	0.038
Weight (kg)		62.00 (55.00, 70.00)	60.00 (55.00, 68.00)	64.00 (55.00, 70.00)	0.427
Height (cm)		166.00 (160.00, 172.00)	166.00 (160.00, 171.50)	166.50 (160.00, 173.00)	0.394

Data were presented as N(%) or median (IQR). pT, pathological T stage; pN, pathological N stage; pTNM, pathological tumor-node-metastasis stage; WBC, white blood cell; LYM, lymphocyte; NEU, neutrophil; MONO, monocyte; EOS, eosinophil; BASO, basophil; RBC, red blood cell; HGB, hemoglobin; HCT, hematocrit; MCV, mean corpuscular volume; MCH, mean corpuscular hemoglobin; MCHC, mean corpuscular hemoglobin concentration; RDW, red cell distribution width; PLT, platelet; MPV, mean platelet volume; PDW, platelet distribution width; PCT, plateletcrit; ALT, alanine aminotransferase; AST, aspartate aminotransferase; γ-GGT, gamma-glutamyl transferase; LDH, lactate dehydrogenase; ALP, alkaline phosphatase; TBIL, total bilirubin; DBIL, direct bilirubin; IDBIL, indirect bilirubin; TP, total protein; ALB, albumin; GLOB, globulin; A/G, albumin/globulin ratio; PALB, prealbumin; GLU, glucose; CREA, creatinine; UA, uric acid; CO<sub>2</sub>-CP, carbon dioxide combining power; K, potassium; Na, sodium; CL, chloride; Ca, calcium; PHOS, phosphorus; Mg, magnesium; CA199, carbohydrate antigen 19-9; CEA, carcinoembryonic antigen; CA724, carbohydrate antigen 72-4; CA125, carbohydrate antigen 125; SG, specific gravity.

### 3.4 Categorization of prediction scores and risk stratification

In the test set, the XGBoost model was used to estimate the 5-year all-cause mortality risk for DGC patients and generate corresponding prediction scores. Patients with prediction scores greater than 0.5576 were classified as the high-risk group, whereas those with scores below 0.5576 were assigned to the low-risk group (Fig. 4A).

The Kaplan-Meier survival analysis revealed a significant difference in 5-year mortality between the two groups (Fig. 4B). Over the 5-year follow-up period, survival rates in the high-risk group declined more rapidly, indicating that higher prediction scores were strongly associated with increased mortality risk.

## 4 Discussion

Patients with DGC generally have a poor prognosis, with several

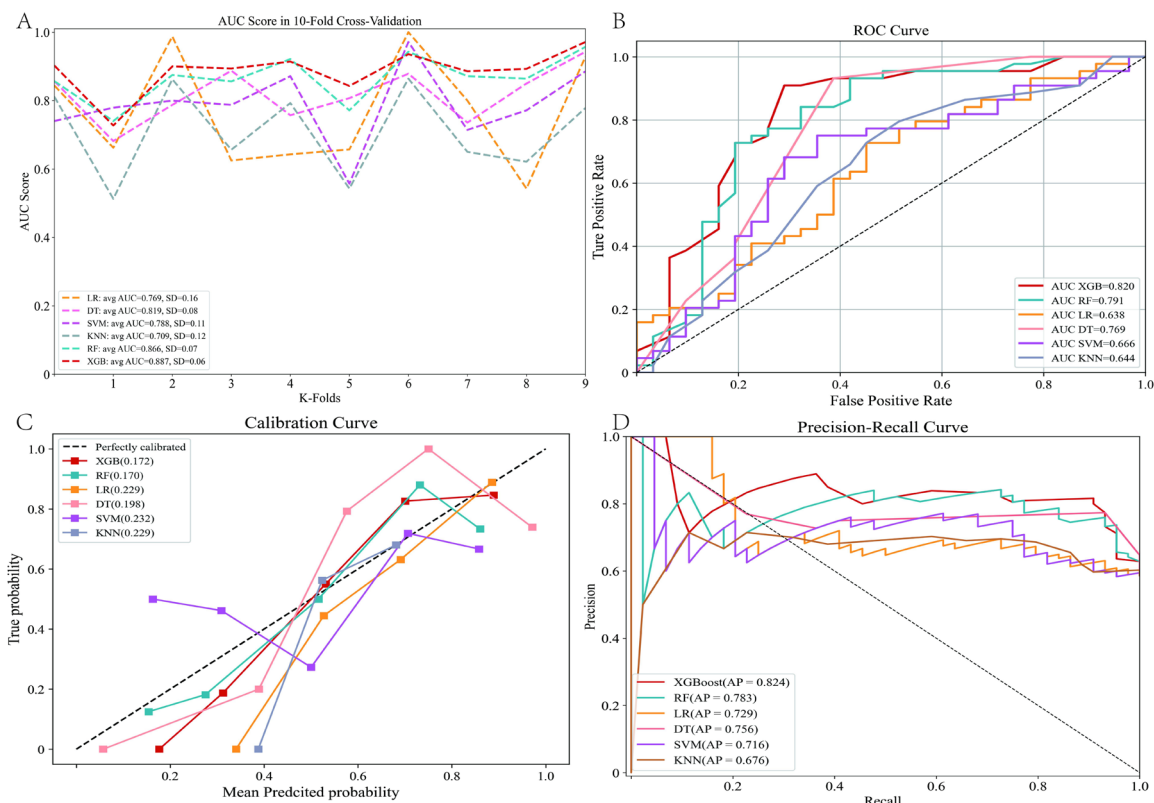


**Fig. 3** Comparison of model performance across six machine learning algorithms. Receiver operating characteristic (ROC) curves for the training set (A) and test sets (B), calibration curves for the test set (C), and precision-recall curves for the test set (D).

**Table 2** Predictive performance of different machine learning models in the test set

Models	AUC (95% CI)	Accuracy	F1 Score	Brier Score
DT	0.769 (0.752-0.787)	0.800	0.781	0.198 (0.191-0.206)
LR	0.638 (0.62-0.653)	0.618	0.498	0.229 (0.226-0.233)
KNN	0.644 (0.625-0.662)	0.667	0.641	0.229 (0.226-0.232)
SVM	0.666 (0.649-0.681)	0.640	0.630	0.232 (0.225-0.238)
RF	0.791 (0.749-0.778)	0.747	0.727	0.170 (0.163-0.176)
XGB	0.820 (0.805-0.833)	0.800	0.781	0.172 (0.166-0.177)

AUC, area under the receiver operating characteristic curve, DT, decision tree, SVM, support vector machine, KNN, k-nearest neighbors, LR, logistic regression, RF, random forest, XGB, extreme gradient boosting.

**Table 3** Predictive performance of different machine learning models in the training set using 10-fold cross-validation

Models	AUC	Accuracy	F1 Score	Brier score
DT	0.819 ± 0.075	0.788 ± 0.089	0.831 ± 0.063	0.165 ± 0.042
SVM	0.788 ± 0.106	0.718 ± 0.088	0.750 ± 0.092	0.188 ± 0.034
KNN	0.709 ± 0.122	0.625 ± 0.115	0.649 ± 0.128	0.221 ± 0.020
LR	0.769 ± 0.156	0.717 ± 0.117	0.791 ± 0.085	0.208 ± 0.038
RF	0.866 ± 0.065	0.811 ± 0.079	0.851 ± 0.059	0.149 ± 0.030
XGB	0.887 ± 0.062	0.789 ± 0.097	0.829 ± 0.074	0.152 ± 0.024

Data were presented as mean ± SD; AUC, area under the receiver operating characteristic curve, DT, decision tree, SVM, support vector machine, KNN, k-nearest neighbors, LR, logistic regression, RF, random forest, XGB, extreme gradient boosting.

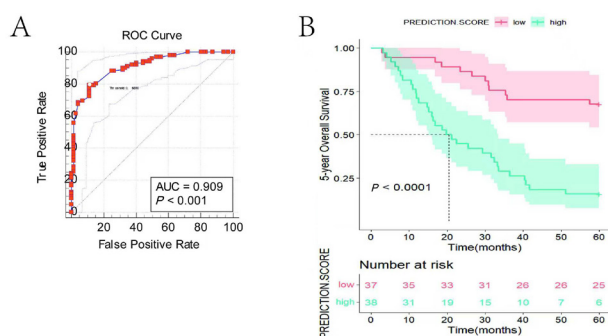


**Fig. 4** Machine learning-based risk prediction model analysis (A) Optimal categorization threshold derived from prediction score; (B) Kaplan-Meier survival curves for patients classified into low-risk and high-risk groups based on the machine learning model.

studies reporting a 5-year survival rate of only 3%-10%<sup>[27]</sup>. Therefore, tailoring treatment strategies based on predicted survival is critical for improving patient outcomes. This study aimed to apply multiple machine learning models to predict the 5-year all-cause mortality of DGC patients in extremely cold regions and to compare the predictive capabilities of these models

in order to identify the best-performing approach.

To our knowledge, this is the first study to use machine learning to predict 5-year all-cause mortality in a large cohort of DGC patients from extremely cold regions. The findings suggest that unique climatic characteristics of such regions may influence GC progression and prognosis, altering clinical features and biomarker profiles. Although numerous factors affect GC development and outcomes, traditional TNM staging still exhibits certain limitations in accurately guiding treatment decisions<sup>[28-29]</sup>. With the rise of precision medicine, more sensitive and comprehensive prognostic tools are needed to improve risk stratification for DGC patients in extremely cold environments.

Previous studies have explored the use of machine learning in oncology<sup>[30-32]</sup>. For instance, Turkki *et al.* utilized artificial neural networks and support vector machines to predict breast cancer prognosis<sup>[33]</sup>. Their model used tumor recurrence (local and systemic) and cancer-related mortality within 32 months as outcome variables. In the field of Barrett's esophagus, machine learning approaches have enhanced automated quantification of Cytosponge-TFF3 glandular structures, achieving strong performance (class-balanced accuracy of 0.77)<sup>[34]</sup>, while Gehrung *et al.* developed a fully automated deep-learning system for reading Cytosponge-TFF3 samples, although its sensitivity remained lower than manual reading (72.6% vs. 81.7%)<sup>[35]</sup>.

In this study, we constructed an ML-based risk stratification model to predict 5-year all-cause mortality in DGC patients from extremely cold regions. Missing values were imputed using the KNN imputer, predictive variables were selected using RFE, and 10-fold cross-validation was applied to reduce overfitting and enhance model robustness. Among the six evaluated models, XGBoost demonstrated the strongest classification performance. Its core principle involves iteratively reducing model bias by fitting new base learners to the residuals of previous models, thereby improving predictive stability and accuracy<sup>[36]</sup>. Comprehensive analysis of clinical data showed that XGBoost achieved the highest AUC values in both the training set (0.887) and the test set (0.820), as well as the highest F1 scores (0.830 vs. 0.781). It also attained the second-best Brier score (0.172). Together, these metrics demonstrate that XGBoost can efficiently and accurately predict the 5-year all-cause mortality for DGC patients in extremely cold regions, highlighting the potential and applicability of machine learning for GC prognosis assessment.

This study provides several clinical implications. First, the machine learning models, particularly XGBoost, exhibited excellent predictive performance for DGC outcomes in extremely cold regions. The identified predictive features—pT, pN, pTNM, LYM, RBC, ALP, TBIL, CA19-9, CA125, and Borrmann type IV

gastric cancer—are routinely obtainable in clinical practice. Many of these factors (including pT, pN, pTNM, LYM, CA19-9, CA125, and Borrmann type IV gastric cancer) have known associations with GC prognosis, consistent with previous studies<sup>[37-38]</sup>. The model's reliability was further supported through cross-validation and independent testing. These findings suggest that machine learning may serve as a valuable adjunct to traditional clinical assessment, aiding clinicians in accurately identifying high-risk DGC patients in extremely cold regions.

However, this study has limitations. First, it included patients from a single institution, which may introduce selection or information bias. Second, due to the lack of multi-center external validation, we were unable to determine whether the model performs consistently across different extremely cold regions. Third, retrospective design and relatively limited sample size may restrict the generalizability of our findings. Prospective, large-scale, multi-center studies will be essential to further validate the model and improve its predictive robustness. Future research should integrate additional data sources—such as radiomics, histopathology, environmental exposures, and lifestyle factors—to enhance predictive accuracy and deepen understanding of GC prognosis in cold climates.

Overall, this study compared multiple machine learning models and found that XGBoost demonstrated the best performance in predicting 5-year all-cause mortality for DGC patients living in extremely cold regions. Despite its limitations, the work provides important insights and establishes a foundation for further development of precision prognostic tools in GC.

## 5 Conclusion

This study is the first to apply machine learning models to predict the 5-year all-cause mortality rate in DGC patients from extremely cold regions. The XGBoost model showed the strongest predictive performance, with the highest AUC and F1 values and a comparatively low Brier score. These findings highlight the potential of machine learning to improve prognosis assessment for DGC in distinctive environmental setting. Future research should focus on validating these findings across multiple centers and further exploring region-specific risk factors and preventive strategies to improve GC outcomes in extremely cold areas.

## Acknowledgements

The authors gratefully acknowledge the Harbin Medical University Cancer Hospital for providing the clinical data used in this study.

## Research ethics

This study was conducted in accordance with the principles of

the Declaration of Helsinki and was approved by the Medical Ethics Committee of Harbin Medical University Cancer Hospital (KY2021-09).

## Informed consent

Informed consent was obtained from all patients prior to treatment.

## Author contributions

Zhang Y L and Wang C designed and conceptualized the study, drafted the manuscript, and contributed equally to this work. Zhang Y L, Wang C, Fan J L and Gao H Y were responsible for data collection. Zhu X Q and Song H B conducted the final critical review of the manuscript. All authors contributed to the article and approved the final submitted version.

## Use of large language models, AI and machine learning tools

No large language models or AI-assisted writing tools were used

in the preparation of this manuscript.

## Conflict of interests

All authors declare that they have no conflicts of interest related to this study.

## Research funding

This research was supported by the Fund for Independent Innovation of Hypoglycemic Drugs from Basic Research to Clinical Application (070500020373) and Heilongjiang Provincial Natural Science Foundation (PL2025H169).

## Data availability

Patient data were stored in the Gastric Cancer Information Management System v1.2, developed by the Harbin Medical University Cancer Hospital (Copyright No. 2013SR087424, <http://www.sghmu.com>).

## References

- [1] No authors listed. Erratum: Global cancer statistics 2018: GLOBOCAN estimates of incidence and mortality worldwide for 36 cancers in 185 countries. *CA Cancer J Clin*, 2020; 70(4): 313.
- [2] Brenner H, Rothembacher D, Arndt V. Epidemiology of stomach cancer. *Methods Mol Biol*, 2009; 472: 467-477.
- [3] Thrift A P, Wenker T N, El-Serag H B. Global burden of gastric cancer: epidemiological trends, risk factors, screening and prevention. *Nat Rev Clin Oncol*, 2023; 20(5): 338-349.
- [4] Hartgrink H H, van de Velde C J, Putter H, *et al*. Extended lymph node dissection for gastric cancer: who may benefit? Final results of the randomized Dutch gastric cancer group trial. *J Clin Oncol*, 2004; 22(11): 2069-2077.
- [5] Kinoshita T, Uyama I, Terashima M, *et al*. Long-term outcomes of laparoscopic versus open surgery for clinical stage II/III gastric cancer: a multicenter cohort study in Japan (LOC-A Study). *Ann Surg*, 2019; 269(5): 887-894.
- [6] Liu F, Huang C, Xu Z, *et al*. Morbidity and mortality of laparoscopic vs open total gastrectomy for clinical stage I gastric cancer: the CLASS02 multicenter randomized clinical trial. *JAMA Oncol*, 2020; 6(10): 1590-1597.
- [7] Siegel R L, Miller K D, Jemal A. Cancer statistics, 2016. *CA Cancer J Clin*, 2016; 66(1): 7-30.
- [8] Lauren P A. The two histological main types of gastric carcinoma: diffuse and so-called intestinal-type carcinoma: an attempt at a histological classification. *Acta Pathol Microbiol Scand*, 1965; 64(1): 31-49.
- [9] Chen Y C, Fang W L, Wang R F, *et al*. Clinicopathological variation of lauren classification in gastric cancer. *Pathol Oncol Res*, 2016; 22(1): 197-202.
- [10] Qiu M Z, Cai M Y, Zhang D S, *et al*. Clinicopathological characteristics and prognostic analysis of Lauren classification in gastric adenocarcinoma in China. *J Transl Med*, 2013; 11: 58.
- [11] Li R, Zhang H, Cao Y, *et al*. Lauren classification identifies distinct prognostic value and functional status of intratumoral CD8(+) T cells in gastric cancer. *Cancer Immunol Immunother*, 2020; 69(7): 1327-1336.
- [12] Chandra R, Balachandar N, Wang S, *et al*. The changing face of gastric cancer: epidemiologic trends and advances in novel therapies. *Cancer Gene Ther*, 2021; 28(5): 390-399.
- [13] Richa, Sharma N, Sageena G J T M C. Dietary factors associated with gastric cancer-a review. *Transl Med Commun*, 2022; 7(1): 7.
- [14] Huang B, Liu J, Ding F, *et al*. Epidemiology, risk areas and macro determinants of gastric cancer: a study based on geospatial analysis. *Int J Health Geogr*, 2023; 22(1): 32.
- [15] Deo R C. Machine Learning in Medicine. *Circulation*, 2015; 132(20): 1920-1930.
- [16] Komura D, Ishikawa S. Machine learning approaches for pathologic diagnosis. *Virchows Arch*, 2019; 475(2): 131-138.
- [17] Tran N K, Albahra S, May L, *et al*. Evolving applications of artificial intelligence and machine learning in infectious diseases testing. *Clin Chem*, 2021; 68(1): 125-133.
- [18] Gao Y, Xin L, Lin H, *et al*. Machine learning-based automated sponge cytology for screening of oesophageal squamous cell carcinoma and adenocarcinoma of the oesophagogastric junction: a nationwide, multicohort, prospective study. *Lancet Gastroenterol Hepatol*, 2023; 8(5): 432-445.
- [19] AlJame M, Ahmad I, Imtiaz A, *et al*. Ensemble learning model for

- diagnosing COVID-19 from routine blood tests. *Inform Med Unlocked*, 2020; 21: 100449.
- [20] Okada S, Ohzeki M, Taguchi S. Efficient partition of integer optimization problems with one-hot encoding. *Sci Rep*, 2019; 9(1): 13036.
- [21] Yuan K C, Tsai L W, Lee K H, *et al*. The development an artificial intelligence algorithm for early sepsis diagnosis in the intensive care unit. *Int J Med Inform*, 2020; 141: 104176.
- [22] Nick T G, Campbell K M. Logistic regression. *Methods Mol Biol*, 2007; 404: 273-301.
- [23] Uddin S, Khan A, Hossain M E, *et al*. Comparing different supervised machine learning algorithms for disease prediction. *BMC Med Inform Decis Mak*, 2019; 19(1): 281.
- [24] Jiang H, Mao H, Lu H, *et al*. Machine learning-based models to support decision-making in emergency department triage for patients with suspected cardiovascular disease. *Int J Med Inform*, 2021; 145: 104326.
- [25] Youssef Ali Amer A. Global-local least-squares support vector machine (GLocal-LS-SVM). *PLoS One*, 2023; 18(4): e0285131.
- [26] Salvador-Meneses J, Ruiz-Chavez Z, Garcia-Rodriguez J. Compressed kNN: K-nearest neighbors with data compression. *Entropy (Basel)*, 2019; 21(3): 234.
- [27] Park J C, Lee Y C, Kim J H, *et al*. Clinicopathological aspects and prognostic value with respect to age: an analysis of 3 362 consecutive gastric cancer patients. *J Surg Oncol*, 2009; 99(7): 395-401.
- [28] Fang C, Wang W, Deng J Y, *et al*. Proposal and validation of a modified staging system to improve the prognosis predictive performance of the 8th AJCC/UICC pTNM staging system for gastric adenocarcinoma: a multicenter study with external validation. *Cancer Commun (Lond)*, 2018; 38(1): 67.
- [29] Wang Y, Zhang J, Guo S, *et al*. Implication of lymph node staging in migration and different treatment strategies for stage T2N0M0 and T1N1M0 resected gastric cancer: a SEER population analysis. *Clin Transl Oncol*, 2019; 21(11): 1499-1509.
- [30] Bang C S, Ahn J Y, Kim J H, *et al*. Establishing machine learning models to predict curative resection in early gastric cancer with undifferentiated histology: development and usability study. *J Med Internet Res*, 2021; 23(4): e25053.
- [31] Zhou C, Hu J, Wang Y, *et al*. A machine learning-based predictor for the identification of the recurrence of patients with gastric cancer after operation. *Sci Rep*, 2021; 11(1): 1571.
- [32] Zhou C, Wang Y, Ji M H, *et al*. Predicting peritoneal metastasis of gastric cancer patients based on machine learning. *Cancer Control*, 2020; 27(1): 1073274820968900.
- [33] Turkki R, Byckhov D, Lundin M, *et al*. Breast cancer outcome prediction with tumour tissue images and machine learning. *Breast Cancer Res Treat*, 2019; 177(1): 41-52.
- [34] Wentzensen N, Lahrmann B, Clarke M A, *et al*. Accuracy and efficiency of deep-learning-based automation of dual stain cytology in cervical cancer screening. *J Natl Cancer Inst*, 2021; 113(1): 72-79.
- [35] Gehrung M, Crispin-Ortuzar M, Berman A G, *et al*. Triage-driven diagnosis of Barrett's esophagus for early detection of esophageal adenocarcinoma using deep learning. *Nat Med*, 2021; 27(5): 833-841.
- [36] Wang L, Wang X, Chen A, *et al*. Prediction of type 2 diabetes risk and its effect evaluation based on the XGBoost model. *Healthcare (Basel)*, 2020; 8(3): 247.
- [37] Filik L. Ulcer size and gastric cancer prognosis. *Dig Surg*, 2010; 27(3): 248-249.
- [38] Kemi N, Ylitalo O, Väyrynen J P, *et al*. Tertiary lymphoid structures and gastric cancer prognosis. *Apmis*, 2023; 131(1): 19-25.